Submitted to Ocean Engineering, April 2002

On the limiting parameters of artificial cavitation applied to reduce drag

Konstantin Matveev

California Institute of Technology
MC 301-46
Pasadena, CA 91125
Fax: (626) 395-8469
matveev@caltech.edu

Abstract

Artificial cavitation, or ventilation, is produced by releasing gas into liquid flow. One objective of creating such a multiphase flow is to reduce frictional and sometimes wave resistance of a marine vehicle completely or partially immersed in the water. In this paper, flows around surface ships moving along the water-air boundary are considered. It is favorable to achieve a negative cavitation number in the developed cavitating flow under the vessel's bottom in order to generate additional lift. Cavities formed in the flow have limiting parameters that are affected by propulsive and lifting devices. Methods for calculating these influences and results of a parametric study are reported.

1. Introduction

One of the classes of the boundary layer control is the creation of a multiphase flow by injecting air into liquid flow. It is known that artificially developed cavitating flows effectively reduce drag on surface ships (Matveev, 1999) and underwater rockets (Ashley, 2001). In the case of a surface vessel, called an Air Cavity Ship (ACS), air is supplied under the bottom of special profile so that a steady air bubble is generated, which separates a part of the hull surface from contact with water reducing hydrodynamic resistance. The conceptual scheme is given in Fig. 1, where the important parameters of the longitudinal hull geometry are shown. Pressure inside the cavity, filled with air, is higher than atmospheric. Different from hovercraft and Surface Effect Ships, an ACS does not have flexible skirts, and its rigid bottom sections render a forming action on the cavity shape. Consumption of air needed for supporting the cavity on a properly designed ACS is around 2% from the power used for propulsion; and achieved drag reduction is about 15-30%. Taking into account other positive features, such as low cost, small draught, and easy maintenance, it can be concluded that ACS is a very promising concept in the family of high-performance marine vehicles.

The idea of drag reduction by supplying air to the wetted hull surfaces was proposed in the 19th century. However, most attempts to implement it have failed. Despite a deceptive simplicity of the idea, it is not possible to create a stable cavity at low air injection rate without deep physical understanding of the

phenomenon. Systematic research started in Russia in the 1960's (Butuzov et al., 1990) and resulted in the current serial production of commercial and military ACS with displacement up to 100 tons (Fig. 2) and underwater rockets with artificial cavitation. A review of several air lubrication developments and a dimensional analysis of a planning ACS are given by Latorre (1997).

The nature of the cavitating flow aimed at reducing drag can be understood from an example of the ventilation behind a wedge attached to the horizontal wall in the presence of gravity (Fig. 3). The characteristic feature of shape 1 is the formation of a pulsating reverse jet in the tail part of the cavity, while the cavity boundary close to the wedge remains stable. Cavity 2 is associated with a flow mode when no reverse jet is present, and the tail of the cavity attaches smoothly to the plate. In this case, the cavity-maintaining gas flow as well as cavitation drag is theoretically equal to zero. The peculiarity of cavity 3 is that in theory it pierces the plate at its aft end (as shown by a dash line). During tests, strong pulsations are observed all over the cavity. This regime is realized at high gas consumption. The formation of an unclosed cavity 4 is also possible at certain conditions; however, the power needed for air injection is too high to make this regime attractive for practical drag reduction.

Thus, the flow mode, producing cavity 2, is the most promising. As shown by calculations and verified in experiments (Butuzov, 1967), a cavity length is proportional to the square of the flow velocity. Cavity geometrical characteristics and cavitation number, corresponding to this most favorable situation, are called the limiting parameters; and successful ACS's are designed to operate in this regime. If ship length is large and speed is not high enough, the whole bottom of the vessel cannot be covered by a single cavity. That explains unsuccessful attempts to reduce drag by supplying gas through only one nozzle at low speed regimes. Several air cavities must be created on a slow ACS.

One of the difficulties in ACS designing is related to the dependence of the cavity limiting parameters on the influence from a prolusion system and lifting devices, which is difficult to take into account accurately in model testing due to scale effect. In this paper this influence is studied numerically for the simplified configuration of a step on the lower surface of a horizontal wall. Choosing properly locations and characteristics of the propulsive and lifting devices when designing an ACS, it is possible to achieve high performance of a full-scale vessel.

2. Mathematical Formulation

A two-dimensional cavitating flow around a wedge on the lower side of the horizontal wall is considered (Fig. 4), following Butuzov (1967). A generalized Ryabushinsky scheme is applied: a closing fictitious contour is introduced at the cavity tail. Liquid is assumed to be ideal and incompressible; flow is potential and steady. Pressure in the cavity, including its boundary, is assumed to be uniform and equal to p_c. From Bernoulli theorem it follows

(1) $$p_c = \frac{\rho U_0^2}{2} + p_0 - \frac{\rho U_c^2}{2} + \rho g y_c ,$$

where p_0 is the pressure in the undisturbed flow at $y = 0$. Eq. (1) can be re-written in the non-dimensional form

(2) $$\sigma = -\frac{2y_c}{Fr^2 b} + \left(\frac{U_c}{U_0}\right)^2 - 1,$$

where σ is the cavitation number and Fr is the Froude number, defined by expressions

(3) $$\sigma = \frac{p_0 - p_c}{\rho U_0^2 / 2},$$

(4) $$Fr = U_0 / \sqrt{gb} .$$

Cavities applied for drag reduction are usually thin, so Eq. (2) can be linearized

(5) $$\frac{\sigma}{2} = -\frac{y_c}{Fr^2 b} + \frac{u_c}{U_0},$$

where u_c is the velocity perturbation. In the linear theory, a wedge and a cavity can be simulated by distribution of sources with intensities proportional to the derivative of the obstacle ordinate

(6) $$q(x) = 2U_0 y' .$$

Velocity perturbations, induced by the sources, are computed by formula

(7) $$u = -\frac{1}{2\pi} \int_{-b}^{l+b} \frac{q(\xi) d\xi}{\xi - x} .$$

Combining Eqs. (5-7), a final equation for the cavity shape η_1 is

(8) $$\frac{y_c(x)}{Fr^2 b} + \frac{1}{\pi} \int_0^l \frac{\eta'_1(\xi) d\xi}{\xi - x} d\xi = -\frac{\sigma}{2} + F_{cont}(x) + F_{dist}(x) ,$$

where

(9) $$F_{cont}(x) = -\frac{1}{\pi} \int_{-b}^{0} \frac{\eta'_0(\xi) d\xi}{\xi - x} d\xi - \frac{1}{\pi} \int_l^{l+b} \frac{\eta'_2(\xi) d\xi}{\xi - x} d\xi ;$$

η_0 and η_2 are the ordinates of the main (wedge) and closing contours respectively. $F_{dist}(x)$ is the disturbance induced by singularities representing other objects in the flow, such as propulsive and lifting devices. When their sizes are small in comparison with other characteristic lengths in the problem, these devices can be approximately modeled by hydrodynamic singularities: a sink for a water-jet inlet, a dipole for a propeller, and a vortex for a hydrofoil. It is assumed that a propeller and a water-jet inlet are positioned on the wall line; and a lifting surface is located below the wall. Components of $F_{dist}(x)$ are expressed as follows:

(10) $$F_{source}(x) = \frac{1}{2\pi U_0} \frac{q_1}{x_1 - x} ;$$

(11) $$F_{dipole}(x) = \frac{1}{2\pi U_0} \frac{d}{(x_1 - x)^2} ;$$

(12) $$F_{vortex}(x) = \frac{\gamma}{\pi U_0} \frac{y_1}{(x - x_1)^2 + y_1^2};$$

where q_1, d and γ are the strengths of the singularities, x_1 and y_1 are their coordinates. In a vortex case, a mirror effect is taken into account.

Eq. (8) contains an unknown parameter l; besides, the inclination of a fictitious contour to the horizontal axis β is not known in advance. In order to complete the formulation, two additional equations are needed. One is the condition of the closed contour, comprising a cavity and a wedge, is

(13) $$\int_{-b}^{l+b_1} y'(x)dx = 0.$$

Another equation is the equality of inclinations of the cavity and a fictitious wedge at their joint

(14) $$y'(l) = \beta.$$

Thus, a cavitating problem is reduced to the integral-differential equation (8) together with constraint (13) and (14). A numerical procedure for solving this problem is discussed in [9]. Cavity length l is considered as a known parameter; cavitation number σ and angle β are unknown variables. The integration distance is divided on small intervals, where shape of the cavity $\eta_l(x)$ is approximated by second order polynoms. An obtained system of linear algebraic equations is solved numerically.

3. Results and Discussion

On actual Air Cavity Ships the wedge, generating an air cavity, is often a part of the hull with a nearly zero inclination angle, resembling a rearward-facing step (Fig. 5). In order to obtain numerical data for such a configuration, calculations are carried out in the limit $b \to \infty$ keeping the step height constant.

The computed dependences for reduced closure angle $\beta l/h$ and reduced cavitation number $\sigma l/h$ versus reduced cavity length $f = gl/U_0^2$ are shown in Fig. 6. Two values of the fictitious wedge length b_1/l are used: 0.01 and 0.1. Different closing contours produce significantly different closing angles in the regimes distant from the limiting case (when $\beta=0$). This discrepancy at low f can be attributed to the presence of the reverse jet (Fig. 7). The smaller a fictitious contour is selected, the higher the value of a closing angle. When a limiting regime is obtained, it appears that the length of the cavity does not depend on the size of the fictitious contour, because the closing angle is zero in both cases. Therefore, the results of the modeling aimed at finding the limiting parameters are not sensitive to the choice of a closing wedge.

Cavitation number, corresponding to the limiting regime, is negative. From Eq. (3) it follows that pressure inside the cavity exceeds pressure in the undisturbed flow, so a lifting force is generated, favorable for surface vessels. The smaller closing angle β, the less is the amount of the air escaping from the cavity (Gurevich, 1979), and, consequently, a power needed for air injection. In the limiting regime, this angle is zero, so is a theoretical air flow rate needed to maintain the air cavity.

The theory applied in this study was verified by the experiments for the wedge of a finite angle α (Butuzov, 1967). Figure 8 demonstrates the comparison between experimental data and numerical results for the non-dimensional combinations of cavitation number, reduced wedge length $f_1=gb/U_0$, Froude number based on cavity length $Fr_1^2=U_0^2/gl$, and cavity thickness. The agreement is satisfactory, accounting for the strong assumptions imposed. Experiments do show that the air flow rate in the limiting regime is very small. A gas is escaping from the cavity through two narrow strings at the lateral sides of the cavity; that is a three-dimensional effect, which cannot be modeled by the two-dimensional theory considered here. Significant increase of the air supply in the limiting regime does not practically modify the area covered by the cavity. On the contrary, in the regime distant from the limiting, e.g., when no cavity is present and air is started to be supplied to rear side of the wedge at a fixed flow velocity, a high air flow rate is required to achieve a limiting cavity, since a strong reverse jet is present when a cavity length is much lower than a limiting one.

It happened in the shipbuilding that after a successful testing of a model with an air cavity (but without a propulsor and a control ride system) a full-scale vessel did not deliver the expected performance, namely the air cavity characteristics (area covered, air flow rate, and cavitation number) were not as good as found at the model scale; such a case is mentioned by Tudem (2002). The most probable reason is the negative influence of a propulsor on the cavitating flow. This effect can be estimated within the present model: the dipole resembles the propeller action, and the sink corresponds to the water-jet inlet. The dipole and sink disturbances are introduced via Eqs. (10) and (11). In this study they are located on the wall line behind the cavity, and their non-dimensional intensities, q_1/U_0h and d/U_0lh, are taken to be one. For practical purposes a limiting cavity is of the most importance. The dependences of the reduced cavity length and cavitation number on the location of singularities are shown in Fig. 9. As one can see, positioning the propulsor close to the cavity aft end may significantly degrade the air cavity performance, namely reduce the limiting length and the pressure inside the cavity. For considered intensities of singularities, their influence is small at the distance from the cavity end equal to one cavity length. This is in accordance with the observations when an incorrectly positioned propulsor can suck a significant portion of the cavity. Using mathematical modeling, this effect can be estimated on the design stage, and special measures can be taken to minimize negative interactions between an air cavity and a propulsor.

At the present time hydrofoils are a popular means in the ride control and lift enhancing systems on advanced marine vehicles. The proper application of both hydrofoils and artificial cavitation on one vessel can enhance its performance. In this paper, the influence from a vortex, simulating a hydrofoil, on the air cavity characteristics is studied. The vortex disturbance is expressed via Eq. (12), its vertical coordinate is chosen to be equal to $y_1=0.2l$, and its reduced circulation is $\gamma/U_0h=0.5$. The horizontal coordinate and a sign of a circulation are the variable parameters. A positive circulation corresponds to the clock-wise case. The vortex is positioned in front of, along and behind the cavity. The results for the reduced cavity length and cavitation number are given in Fig. 10. The location of a positive vortex near the wedge is followed by a profound growth of the limiting cavity length and a little increment of the cavity pressure. When a

positive vortex is positioned closer to the cavity aft end, a cavity length becomes much smaller than an undisturbed value, accompanied by a large drop of the cavity pressure. The effect from the vortex of a negative circulation is opposite.

It seems favorable to put a hydrofoil with a positive circulation in the vicinity of the wedge, since in this case both the limiting cavity length and cavity surplus pressure increase, and a hydrofoil produces an upward force. However, on a fast ACS the flow velocity is usually high enough to create a large air cavity covering a significant portion of the hull, so the increase of the limiting length is not important. The positioning of a hydrofoil with negative circulation under the downstream half of the cavity significantly enhances the pressure in the cavity, so a naval architect must make sure that the hydrofoil-cavity system, delivering the best total performance, is selected.

In the case of a relatively slow cargo ship, a cavity length is of great importance, since it defines the number of wedges employed and the overall hull area covered by air cavities. A hydrofoil with a positive circulation located under the first half of the cavity and one with a negative circulation in the second half produce significant enlargement of the cavity. The total effect is again calculated taking into account the forces on a hydrofoil and the change of the cavity pressure. Notice that a hydrofoil is treated as a vortex in this paper; in reality, when its chord is comparable with the distance to the hull and cavity boundary, this approximation may produce significant errors, and a more appropriate distribution of sources and vortices, simulating a hydrofoil, is required for accurate estimations.

4. Conclusions

The influence of singularities, simulating a propulsor and lifting surfaces, on the limiting parameters of a cavity formed under the bottom of a surface vessel are studied within a two-dimensional linearized model for an ideal liquid. It was found that the results for the limiting cavity are not sensitive to the size of a fictitious closing contour located at the aft end of the cavity. Propulsion units, located in the vicinity of the cavity end, negatively affect cavity characteristics. The influence from a hydrofoil, located under the cavity, depends on its horizontal location. The control strategies of artificially cavitating flows by proper hydrofoil positioning are discussed for Air Cavity Ships operating in fast and slow regimes.

References

Ashley, S., May 2001. Warp drive underwater. Scientific American.

Butuzov, A.A., 1967. Artificial cavitation flow behind a slender wedge on the lower surface of a horizontal wall. Fluid Dynamics, 3, 56-58.

Butuzov, A.A., Gorbachev, Y.N, Ivanov, A.N., Kalyuzhny, V.G., and Pavlenko, A.N., 1990. Reduction of ship resistance using ventilated gas cavities. Shipbuilding, 11, 3-6.

Gurevich, M.I., 1979. Jet Theory, Nauka, Moscow.

Latorre, R., 1997. Ship hull drag reduction using bottom air injection. Ocean Engineering, 24, 161-175.

Matveev, K.I., 1999. Modeling of vertical plane motion of an air cavity ship. Proceeding of Fifth International Conference on Fast Sea Transportation. Seattle, WA.

Tudem, U.S., 2002. The challenge of introducing innovative Air Lifted Vessels to the commercial market. Proceedings of Eighteenth Fast Ferry Conference. Nice.

Figure Captions

Fig. 1 Air cavity formed under the bottom of a fast ACS.

Fig. 2 Landing boat Serna using air lubrication.

Fig. 3 Ventilated flow behind a wedge.

Fig. 4 Scheme of the cavitating flow.

Fig. 5 Limiting cavitating flow behind a step.

Fig. 6 Dependences of closure angle (a) and cavitation number (b) on reduced cavity length for two values of the reduced length of a fictitious wedge: (o) – $b_1/l = 0.1$; (Δ) – $b_1/l = 0.01$.

Fig. 7 Flow in the vicinity of the cavity tail at low f.

Fig. 8 Comparison of experimental (dashed line) and theoretical (solid line) results for non-dimensional combinations characterizing cavitation number and cavity length and thickness; adopted from Butuzov (1967).

Fig. 9 Dependence of cavity length (a) and cavitation number (b) on sink (o) and dipole (Δ) locations.

Fig. 10 Dependence of cavity length (a) and cavitation number (b) on a vortex location of a positive (o) and negative (Δ) circulation.

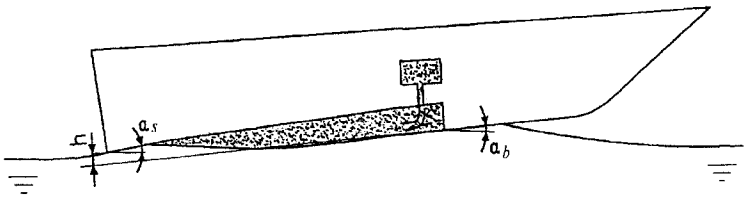

Fig. 1

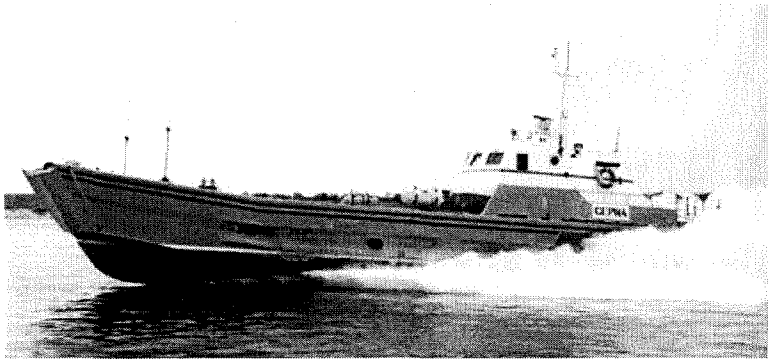

Fig. 2

K. Matveev, 2002, "On the limiting parameters of artificial cavitation applied to reduce drag"

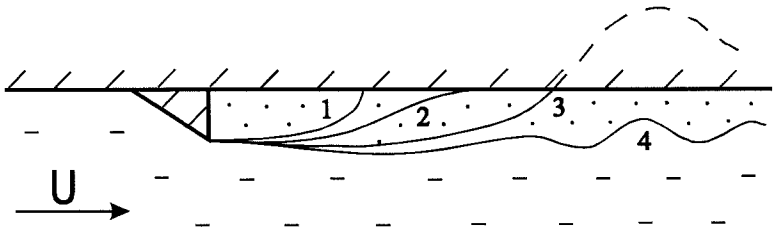

Fig. 3

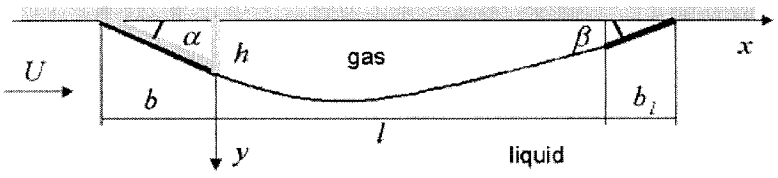

Fig. 4

K. Matveev, 2002, "On the limiting parameters of artificial cavitation applied to reduce drag"

Fig. 5

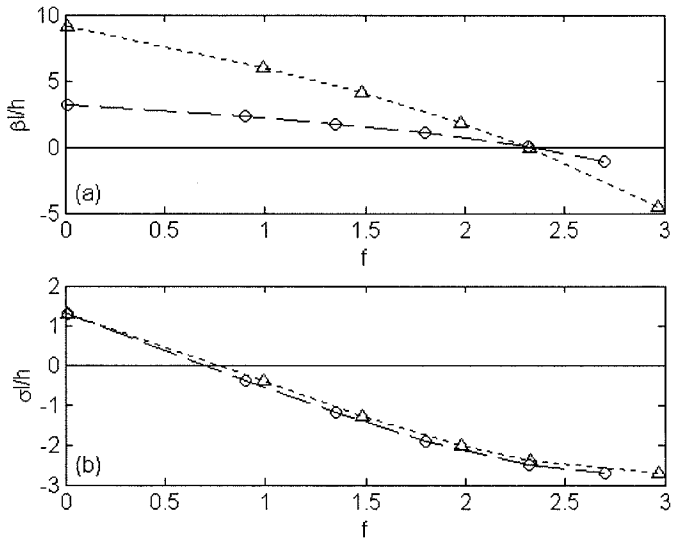

Fig. 6

K. Matveev, 2002, "On the limiting parameters of artificial cavitation applied to reduce drag"

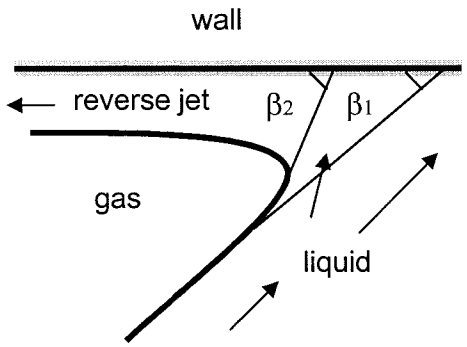

Fig. 7

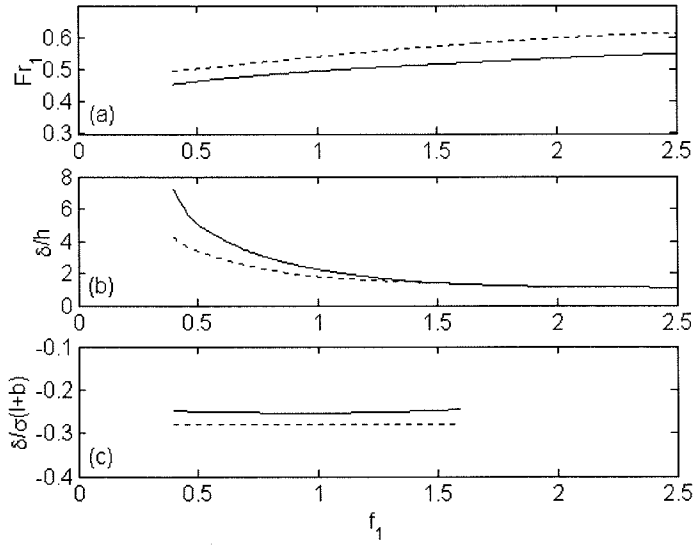

Fig. 8

K. Matveev, 2002, "On the limiting parameters of artificial cavitation applied to reduce drag"

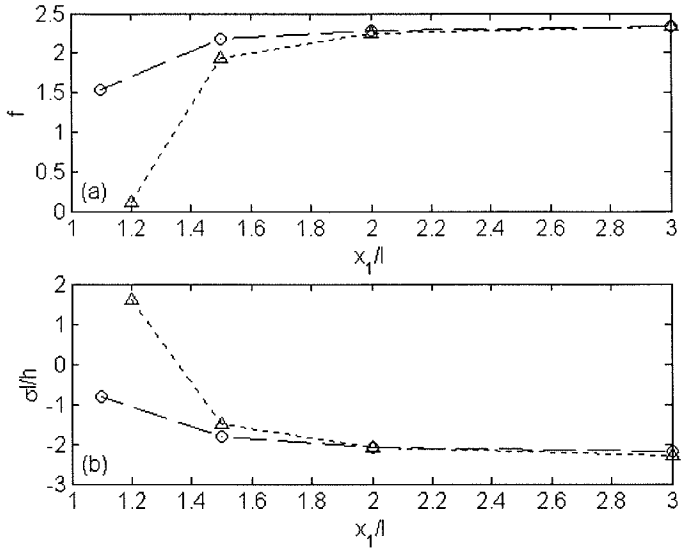

Fig. 9

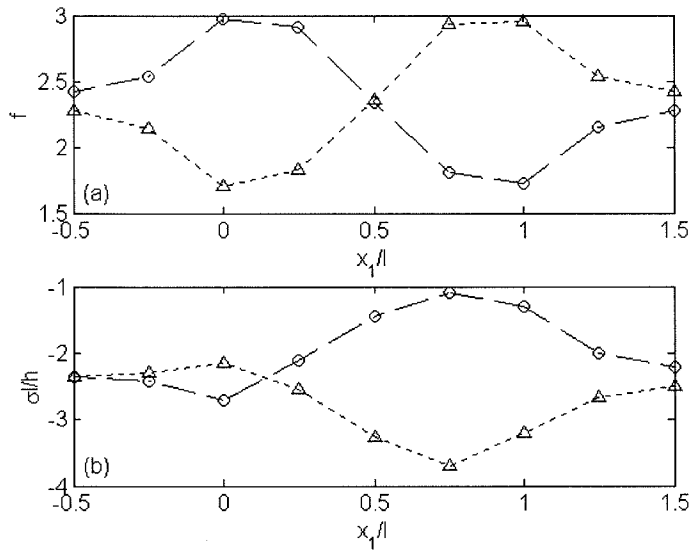

Fig. 10

K. Matveev, 2002, "On the limiting parameters of artificial cavitation applied to reduce drag"